Chapter 8

Neimark-Sacker Bifurcation of a Nonstandard Discretized 3D Tigan System

Fatma Iscan[1], Mevlüde Yakıt Ongun[2]

Abstract

This paper presents a comprehensive qualitative investigation into the discrete-time topological transitions and localized phase space dynamics of a three-dimensional T-system. Crucially, rather than employing a conventional Euler discretization scheme, which frequently induces numerical instabilities and unphysical divergence, the continuous-time vector field is systematically mapped into a discrete layout using a non-local Non-Standard Finite Difference framework. Following the formulation of the rational map, the local topological architecture of the system is rigorously investigated at both the trivial equilibrium and the non-trivial interior equilibrium zones.

The primary objective of this work is to establish the precise boundaries governing the emergence of Neimark-Sacker bifurcations. To achieve this, the explicit algebraic Flip and Neimark-Sacker bifurcation criteria is implemented, which bypasses traditional approximation limits by acting directly on the transcendental characteristic polynomials of the system matrices. Under specific parameter configurations, a scheme-induced supercritical Neimark-Sacker bifurcation artifact is exposed at the origin, evaluated via three-dimensional center manifold projections and complex normal form operators. Conversely, under the physical regime, the stability boundaries shift to the interior manifold, revealing a non-degenerate supercritical Neimark-Sacker bifurcation. The same procedure is implemented to the positive fixed point.

All theoretical analyses are seamlessly supported by comprehensive numerical experiments. Finally, high-density bifurcation diagrams and detailed phase space portraits are provided to visually confirm the structural evolution of the trajectories, capturing the birth, contraction, and expansion of the bifurcated discrete manifolds and invariant closed curves.

Keywords: 3D Tigan System, Non-Standard Finite Difference, Yao Explicit Criteria, Neimark-Sacker Bifurcation, Center Manifold Projection, Phase Portraits, Bifurcation Diagrams.

1 Cand.PhD, Graduate School of Natural and Applied Sciences, Süleyman Demirel University, d2040110342@ogr.sdu.edu.tr, Lecturer, Mehmet Akif Ersoy University, mail fatmaiscan@mehmetakif.edu.tr, ORCID ID:0009-0000-9409-8368

2 Prof. Dr, Süleyman Demirel University, mail mevludeyakit@sdu.edu.tr, ORCID ID:0000-0003-2363-9395

https://doi.org/10.58830/ozgur.pub1361.c5498

1. Introduction

Dynamical systems theory constitutes an indispensable mathematical foundation for analyzing, predicting, and controlling the evolution of time-dependent phenomena across a wide spectrum of scientific engineering fields, such as fluid mechanics, population biology, secure communication protocols, and aerospace control networks. Fundamentally, a mathematical description of a real-world physical configuration naturally arises in the form of continuous-time autonomous differential equations. In these continuous frameworks, the primary objective is to characterize the qualitative and topological structures of the phase space, which are strictly governed by geometric invariants such as vector fields, manifolds, and trajectories. However, characterizing non-linear continuous systems presents massive analytical difficulties, as most realistic multi-dimensional models resist exact closed-form integrations. Consequently, researchers must rely heavily on localized linearizations, qualitative geometric theories, and advanced bifurcation analyses to map out long-term asymptotic behaviors and topological transitions [11], [12], [14], [15], [18], [21].

A profound paradigm shift in computational and theoretical non-linear dynamics occurs when transitioning from continuous-time vector fields to discrete-time mappings. In modern computational science, this temporal transition is not merely a matter of convenience but a fundamental prerequisite. Real-time digital signal processing, numerical simulators, and micro-controller-based modern engineering designs operate strictly on discrete temporal iterations rather than continuous time intervals. Nevertheless, this discretization process introduces severe theoretical complications and numerical anomalies due to the divergence in topological constraints between the two domains [12], [15], [21], [27], [28], [29], [30]. For instance, according to the classical Poincaré-Bendixson theorem, continuous autonomous systems require a minimum of three dimensions to exhibit chaotic or strange attractors. Discrete maps, however, are entirely liberated from such dimensional restrictions; they can display highly complex, chaotic trajectories and topological entanglements even within one or two dimensional phase spaces [2].

As a consequence of this fundamental difference, transforming a continuous-time system into a discrete counterpart can severely alter the underlying structural invariants. Classical numerical schemes, most notably the forward explicit Euler method, are notorious for introducing severe numerical artifacts. At larger iteration steps, these standard methods frequently induce non-physical chaotic oscillations, artificially shift or destroy the localized stability boundaries of equilibria, or introduce spurious fixed points that possess no physical meaning in the parent continuous-time model. To overcome these fundamental qualitative deficiencies, the application of the Non-Standard Finite Difference (NSFD) method, pioneered by Mickens, has emerged as a mathematically superior discretization paradigm. By utilizing sophisticated non-local approximations for non-linear terms and designing parameter-dependent complex denominator

functions, the NSFD framework meticulously preserves the structural invariants of the continuous-time system, such as positivity of solutions, boundedness, and elementary stability profiles, regardless of the chosen step size [3], [8], [9], [16], [17].

A significant milestone in modern chaotic dynamics within this domain was achieved by Tigan (2005), who introduced a novel three-dimensional autonomous chaotic system, widely recognized in the literature as the Tigan system or 3D T-system, which is governed by the following set of ordinary differential equations:

$$\begin{aligned} \dot{x} &= a(y - x) \\ \dot{y} &= (c - a)x - axz \\ \dot{z} &= xy - bz \end{aligned} \tag{1}$$

where a, b and c represent positive real parameters. Despite its apparent algebraic simplicity, the Tigan system exhibits an extraordinarily rich topological structure, including complex butterfly-shaped strange attractors, multiple coexisting global bifurcations, and complex manifold structures [23]. While the continuous Tigan system and its classical Euler-discretized variants have been partially explored in literature [20], the systematic discrete-time bifurcation analysis of the Tigan system under a structurally preserved NSFD discretization scheme remains completely unaddressed. Motivated by this distinct research gap, this paper constructs the non-standard discrete-time mapping of the 3D Tigan system by strictly applying Mickens' design rules, yielding the following discrete formulation:

$$\begin{aligned} x_{n+1} &= \frac{1}{1+\varphi a}\left(x_n + a\varphi\, y_n\right) \\ y_{n+1} &= y_n + \left((c - a)x_n - ax_n z_n\right) \\ z_{n+1} &= \frac{1}{1+\varphi b}\left(z_n + \varphi\, x_n y_n\right) \end{aligned} \tag{2}$$

where a, b and c represent the positive continuous system parameters, and $\varphi > 0$ is the non-standard step-size denominator function, which serves as our primary bifurcation parameter throughout this work.

When stable discrete-time systems like the proposed NSFD Tigan system map encounter variations in their parameter space, they face structural instabilities known as bifurcations, where the qualitative nature of the phase space shifts abruptly. In multi-dimensional discrete maps, the primary routes to deterministic chaos are governed by the Flip (period-doubling) and Neimark-Sacker (discrete Hopf) bifurcations. The rigorous classification of these discrete instabilities traditionally requires calculating the exact spectrum (eigenvalues) of the

localized Jacobian matrix and implementing intricate center manifold reductions based on classical projection methods [11]. However, in multi-parameter spaces or systems exhibiting coupled block-diagonal structures, computing exact complex eigenvalues analytically becomes highly tedious or introduces severe numerical singularities. To resolve this computational bottleneck, advanced algebraic frameworks have been developed to evaluate bifurcation criteria explicitly from the coefficients and invariants of the system's characteristic equation, completely bypassing the direct computation of eigenvalues and baseline eigenvectors [4], [5], [6], [7], [10], [11], [13], [19], [24], [25], [26], [30].

The primary novelty and contribution of this work lie in evaluating the NSFD-discretized Tigan system map using the explicit, eigenvalue-free algebraic bifurcation criteria proposed by Yao (2012). A mathematically transparent bridge is established to analyze the localized dynamics and structural stability around the fixed points. By doing so, we explicitly demonstrate how the NSFD scheme structurally outperforms classical Euler discretizations by maintaining strict topological alignment with the continuous Tigan system, while providing closed-form analytical solutions for the first Lyapunov coefficient on the reduced center manifold.

The remainder of this paper is structured as follows. In Section 2, the fixed points of the NSFD Tigan system map are established, and localized linear stability is evaluated via the Jacobian operator. Section 3 is dedicated to the application of the explicit bifurcation criteria and the analytical formulation of the center manifold reduction. Section 4 provides the corresponding numerical simulations, phase portraits, and maximum Lyapunov exponent (MLE) graphs to visually validate our mathematical proofs. Finally, a brief conclusion and future research horizons are presented in Section 5.

2. Local Stability Analysis of Fixed Points

In this section, the fixed points of the discrete-time NSFD Tigan map are characterized, and their local asymptotic stability is examined through a rigorous linear algebraic framework.Setting the right-hand side of system (2) equal to zero yields the following system of nonlinear equations, whose solutions correspond to the equilibrium points of the system:

$$\begin{aligned} x &= \frac{x+a\varphi y}{1+\varphi a} \\ y &= y + \varphi((c-a)x - axz) \\ z &= \frac{z+\varphi xy}{1+\varphi b} \end{aligned} \tag{3}$$

The following lemma can be established through direct algebraic computations.

Lemma 1: For any parameter values, the system (2)

(i) has a unique fixed point given by $E_0(0,0,0)$,

(ii) If $c > a$, system (2) possesses three fixed points $E_1(0,0,0), E_{2,3} = \left(\pm\sqrt{\frac{b(c-a)}{a}}, \pm\sqrt{\frac{b(c-a)}{a}}, \frac{c-a}{a}\right)$.

Performing the analytical differentiation on NSFD formulation yields the following the Jacobian matrix and the characteristic equation given at any fixed point $E(x,y,z)$ are obtained as:

$$J(E) = \begin{pmatrix} \frac{1}{a\varphi+1} & \frac{a\varphi}{a\varphi+1} & 0 \\ \varphi(-az-a+c) & 1 & -a\varphi x \\ \frac{\varphi y}{b\varphi+1} & \frac{\varphi x}{b\varphi+1} & \frac{1}{b\varphi+1} \end{pmatrix} \tag{4}$$

and

$$P(\rho) \coloneqq \rho^3 + \vartheta_2\rho^2 + \vartheta_1\rho + \vartheta_0 = 0 \tag{5}$$

where

$$\begin{gathered} \vartheta_2 = -tr(J), \\ \vartheta_1 = \begin{vmatrix} j_{11} & j_{12} \\ j_{21} & j_{22} \end{vmatrix} + \begin{vmatrix} j_{22} & j_{23} \\ j_{32} & j_{33} \end{vmatrix} + \begin{vmatrix} j_{11} & j_{13} \\ j_{31} & j_{33} \end{vmatrix}, \\ \vartheta_0 = -|J|. \end{gathered} \tag{6}$$

Firstly, the following lemma establishes the necessary and sufficient conditions for the stability of System (2) around its fixed point, which are used to describe the local dynamics near $E(x,y,z)$.

Lemma 2: Suppose that $\varpi_2, \varpi_1, \varpi_0 \in \mathbb{R}$. Then, the necessary and sufficient conditions for all roots μ of the equation

$$\mu^3 + \varpi_2\mu^2 + \varpi_1\mu + \varpi = 0$$

to satisfy $|\mu| < 1$ are

$|\varpi_2 + \varpi_0| < 1 + \varpi_1, |\varpi_2 - 3\varpi_0| < 3 - \varpi_1$ and $\varpi_0^2 + \varpi_1 - \varpi_0\varpi_2 < 1$ [1], [22].

In this section, the local dynamics of System (2) in a neighborhood of the fixed E_0 are studied in accordance with Lemma 2. The Jacobian matrix at E_0 is given by

$$J(E_0) = \begin{pmatrix} \frac{1}{a\varphi+1} & \frac{a\varphi}{a\varphi+1} & 0 \\ \varphi(-a+c) & 1 & 0 \\ 0 & 0 & \frac{1}{b\varphi+1} \end{pmatrix} \tag{7}$$

The characteristic equation of matrix $J(E_0)$ is

$$P \coloneqq \rho^3 + \kappa_2\rho^2 + \kappa_1\rho + \kappa_0 \tag{8}$$

where,

$$\kappa_2 = -\frac{ab\varphi^2+2a\varphi+2b\varphi+3}{(a\varphi+1)(b\varphi+1)}$$
$$\kappa_1 = \frac{a^2b\varphi^3 - abc\varphi^3 + a^2\varphi^2 - ac\varphi^2 + a\varphi + b\varphi + 3}{(a\varphi+1)(b\varphi+1)} \quad (9)$$
$$\kappa_0 = -\frac{a^2\varphi^2 - ac\varphi^2 + 1}{(a\varphi+1)(b\varphi+1)}$$

The Jacobian matrix $J(E_0)$ have eigenvalues $\rho_1 = \frac{1}{\varphi b+1}, \rho_{2,3} = \frac{1}{2}\left[B \mp \sqrt{B^2-4C}\right]$ where $\mu_{2,3}$ satisfy the equation $\rho^2 - B\rho + C = 0$, where $B = -\frac{a\varphi+2}{1+\varphi a}, C = \frac{a^2\varphi^2-ac\varphi^2+1}{1+\varphi a}$.

So in the following lemma the local stability classification of E_0 presented is obtained:

Lemma 3: If $c < a$ the fixed point $E_0$is a

(i) sink if $-3a^2+4ac \geq 0$ and $\varphi < min\left\{\frac{2}{b}, -\frac{a+\sqrt{-3a^2+4ac}}{a^2-ac}\right\}$ or $-3a^2+4ac < 0$ and $\varphi < min\left\{\frac{2}{b}, \frac{1}{a-c}\right\}$.

(ii) source if $-3a^2+4ac \geq 0$, $\varphi > max\left\{\frac{2}{b}, -\frac{a-\sqrt{-3a^2+4ac}}{a^2-ac}\right\}$ and $-3a^2+4ac < 0$ and $\varphi > max\left\{\frac{2}{b}, \frac{1}{a-c}\right\}$.

(iii) saddle if $-\frac{a+\sqrt{-3a^2+4ac}}{a^2-ac} < \varphi < -\frac{a-\sqrt{-3a^2+4ac}}{a^2-ac}$.

(iv) Non-hyperbolic if

a) $-3a^2+4ac \geq 0, \varphi = \frac{2}{b}$ or $\varphi = -\frac{a\pm\sqrt{-3a^2+4ac}}{a^2-ac}$,

b) $-3a^2+4ac < 0, \varphi = \frac{1}{a-c}$.

Let,

$$NSB_{E_0} = \left\{(a,b,c,\varphi): \varphi = \frac{1}{a-c}, -3a^2+4ac < 0\right\}.$$

If parameters change in small vicinity of NSB_{E_0}, then system (2) meets a Neimark-Sacker bifurcation at E_0.

The Jacobian matrix for E_+ is

$$J(E_+) = \begin{pmatrix} \frac{1}{a\varphi+1} & \frac{a\varphi}{a\varphi+1} & 0 \\ 0 & 1 & -\varphi\sqrt{-ba^2+abc} \\ \varphi\sqrt{\frac{-ba+bc}{a(b\varphi+1)^2}} & \varphi\sqrt{\frac{-ba+bc}{a(b\varphi+1)^2}} & \frac{1}{b\varphi+1} \end{pmatrix} \quad (10)$$

and the characteristic equation of matrix $J(E_+)$ is

$$P := \rho^3 + \kappa_2\rho^2 + \kappa_1\rho + \kappa_0 \tag{11}$$

where,

$$\begin{aligned} \kappa_2 &= -\frac{ab\varphi^2+2a\varphi+2b\varphi+3}{(a\varphi+1)(b\varphi+1)} \\ \kappa_1 &= -\frac{a^2b\varphi^3 - abc\varphi^3 + ab\varphi^2 - bc\varphi^2 - a\varphi - b\varphi - 3}{(a\varphi+1)(b\varphi+1)} \\ \kappa_0 &= -\frac{a^2b\varphi^3 - abc\varphi^3 - ab\varphi^2 + bc\varphi^2 + 1}{(a\varphi+1)(b\varphi+1)} \end{aligned} \tag{12}$$

According to the Lemma 2 following Lemma is written for stability requirement of E_+.

Lemma 4: The fixed point E_+ is locally asymptotically stable if and only if the coefficients $\kappa_2, \kappa_1, \kappa_0$ satisfy

$$|\kappa_2 + \kappa_0| < 1 + \kappa_1, |\kappa_2 - 3\kappa_0| < 3 - \kappa_1 \text{ and } \kappa_0^2 + \kappa_1 - \kappa_0\kappa_2 < 1.$$

3. Analysis of Neimark-Sacker Bifurcation

In this section, the existence, direction, and stability of the Neimark–Sacker bifurcation of System (2) near the fixed points E_0 and E_+ is studied employing the explicit flip and Neimark–Sacker bifurcation criteria, Kuznetsov's normal form method, and center manifold theory, where φ is considered as the bifurcation parameter[11], [24], [26].

3.1. Neimark-Sacker Bifurcation:Existence, Direction and Stability

In this section, topological classification of the codimension-one local bifurcations occurring at the fixed points is presented E_0 and E_+ of the non-standard finite difference Tigan system mapping. To establish analytical closed-form boundaries without executing direct, parameter-dependent complex root extractions, we deploy the explicit algebraic criteria within the setting of the generalized center manifold projection framework [11], [24], [26].

The existence of the Neimark–Sacker bifurcation is established using the explicit flip and Neimark–Sacker bifurcation criteria, as stated in the following lemma [26].

Lemma 5: Consider the following non-dimensional discrete-time dynamical system

$$\aleph_{k+1} = \mathrm{P}_\eta(\aleph_k)$$

where $\eta \in \mathbb{R}$ is regarded as a bifurcation parameter. Let $J(\aleph^*) = (\theta_{ij})_{n\times n}$ denote the Jacobian matrix of P_η evaluated at a fixed point $\aleph^* \epsilon\, \mathbb{R}^n$. The local

dynamical behavior of the system in a neighborhood of $\aleph^*$ is primarily determined by the eigenvalues of $J(\aleph^*)$. $\eta \in \mathbb{R}$ is being taken as a bifurcation parameter. Furthermore, The equation of the Jacobian matrix $J(\aleph^*) = (\theta_{ij})_{n\times n}$ at fixed point $\aleph^* \epsilon\ \mathbb{R}^n$ for P_η is written as follows

$$D_\eta(\lambda) = \lambda^n + \xi_1\lambda^{n-1} + \cdots + \xi_{n-1}\lambda + \xi_n = 0 \tag{13}$$

where $\xi_i = \xi_i(\eta, \upsilon), i = 1,2, \ldots, n$ and υ is being taken as the control parameter unless stated which is to be determined.We define a sequence of determinants $\left(N_i^{\pm}(\eta,\upsilon)\right)_{i=0}^{n}$ with $N_0^{\pm}(\eta,\upsilon) = 1$ which is to be defined as

$$N_i^{\pm} = det(T_1 \pm T_2) \tag{14}$$

where

$$T_1 = \begin{pmatrix} 1 & \xi_1 & \xi_2 & \cdots & \xi_{i-1} \\ 0 & 1 & \xi_1 & \cdots & \xi_{i-2} \\ 0 & 0 & 1 & \cdots & \xi_{i-3} \\ \cdots & \cdots & \cdots & \cdots & \cdots \\ 0 & 0 & 0 & \cdots & 1 \end{pmatrix} \tag{15}$$

$$T_2 = \begin{pmatrix} \xi_{n-i+1} & \xi_{n-i+2} & \cdots & \xi_{n-1} & \xi_n \\ \xi_{n-i+2} & \xi_{n-i+3} & \cdots & \xi_n & 0 \\ \vdots & \vdots & \cdots & \vdots & \vdots \\ \xi_{n-1} & \xi_n & \cdots & 0 & 0 \\ \xi_n & 0 & \cdots & 0 & 0 \end{pmatrix}. \tag{16}$$

Moreover, assuming that the following conditions are satisfied:

(i) $N_{n-1}^{-}(\eta_0,\upsilon) = 0,\ N_{n-1}^{+}(\eta_0,\upsilon) > 0,\ D_{\eta_0}(1) > 1,\ (-1)^n$

$D_{\eta_0}(-1) > 0, N_i^{\pm}(\eta_0,\upsilon) > 0$ for $i = n-3,\ n-5, \ldots, 2(or\ 1)$ when n is odd(or even respectively).

(ii) $\left(\frac{d}{dv}\left(N_{n-1}^{-}(\eta,\upsilon)\right)\right)_{\upsilon=\upsilon_0} \neq 0,$

(iii) $cos\left(\frac{2\pi}{\ell}\right) \neq \delta,$ where $\ell = 3,4,5, \ldots$ and $\delta = 1 - 0.5\, D_{\eta_0}(1)N_{n-3}^{-}(\eta_0,\upsilon) \Big/ N_{n-2}^{+}(\eta_0,\upsilon)$

Therefore, a Neimark–Sacker bifurcation takes place at the critical value η_0.

3.1.1. Neimark-Sacker bifurcation around E_0

Let $\mathcal{G}: \mathbb{R}^3 \times \mathbb{R}^+ \to \mathbb{R}^3$ represent the smooth discrete-time mapping generated by the NSFD scheme. The localized transcendental flow around the invariant hyper-

surface E_0 is completely governed by the spectrum Spec(J(E_0))which corresponds to the roots of the cubic characteristic equation (8). Suppose the parameters $(a, b, c, \varphi) \in NSB_{E_0}$, the eigenvalues of system (2) are :

$$\rho_1 = \frac{1}{\varphi b+1}, \rho_{2,3} = \frac{2+a\varphi \pm i\sqrt{4(1+a\varphi)^2-(2+a\varphi)^2)}}{2(1+a\varphi)} \tag{17}$$

Let $\varphi = \varphi_{NS} = \frac{1}{a-c}$. Obviously,

$$\left|\rho_{2,3}(\varphi_{NS})\right| = \sqrt{\frac{1-a\varphi^2(c-a)}{1+a\varphi}} = 1, \rho_1(\varphi_{NS}) = \frac{a-c}{1+b-c}$$

and

$$\left.\frac{d|\rho_i(\varphi)|}{d\varphi}\right|_{\varphi=\varphi_{NS}} = \frac{a(a-c)}{4a-2c} \neq 0, i = 2,3. \tag{18}$$

Moreover,

$$\frac{a}{a-c} \neq -2, -\frac{3}{2} \tag{19}$$

implies that $\rho_{2,3}^k \neq 1, k = 1,2,3,4$.

To isolate the non-linear dynamics on the critical two-dimensional invariant surface at $\varphi = \varphi_{NS}$ we define a formal projection operator using the bi-orthogonalization framework of [11].

The non-standard map in a localized perturbational vector form around E_0 is expressed as:

$$X = A(\varphi)X + F \tag{20}$$

where $A(\varphi) = J(E_0; \varphi_{NS})$ represent the critical linear operatör and $F = (0, -\frac{\varphi}{2}xz, \frac{\varphi}{2}xy)^T$ with $\varphi = \varphi_{NS}$. The system (15) can be written as

$$X_{n+1} = AX_n + \frac{1}{2}B(X_n, X_n) + \frac{1}{6}C(X_n, X_n, X_n) + O({X_n}^4)$$

where,

$$B(x,y) = \begin{pmatrix} B_1(x,y) \\ B_2(x,y) \\ B_3(x,y) \end{pmatrix}, \; C(x,y,z) = \begin{pmatrix} C_1(x,y,z) \\ C_2(x,y,z) \\ C_3(x,y,z) \end{pmatrix} \tag{21}$$

The symmetric multilinear functions $B: \mathbb{R}^3 \times \mathbb{R}^3 \longrightarrow \mathbb{R}^3$ and $C: \mathbb{R}^3 \times \mathbb{R}^3 \longrightarrow \mathbb{R}^3$are defined, respectively, as follows:

$$B_i(x,y) = \sum_{j,k=1}^{3} \left.\frac{\partial^2 X_i(v,0)}{\partial v_j \partial v_k}\right|_{v=0} x_j y_k, \;\; i = 1,2,3$$

$$C_i(x,y,z) = \sum_{j,k,l=1}^{3} \left.\frac{\partial^2 X_i(\nu,0)}{\partial \nu_j \partial \nu_k \partial \nu_l}\right|_{\nu=0} x_j y_k u_l, \quad i = 1,2,3$$

For the system (15)

$$B(x,y) = \begin{pmatrix} 0 \\ -\frac{\varphi_{NS}}{2}(x_1y_3 + x_3y_1) \\ \frac{\varphi_{NS}}{2}(x_1y_2 + x_2y_1) \end{pmatrix}, \; C(x,y,z) = \begin{pmatrix} 0 \\ 0 \\ 0 \end{pmatrix} \tag{22}$$

Let $q\epsilon\mathbb{C}^3$ be the right eigenvector of $A(\varphi_{NS})$ corresponding to $\lambda_1 = e^{i\theta_0}$, and let $p\epsilon\mathbb{C}^3$be the adjoint left eigenvector of $A^T(\varphi_{NS})$ satisfying $A^T p = e^{-i\theta_0}p$. Due to the uncoupled block tracking along the stable transversal dimension, the exact algebraic structures are parametrized as:

$$q = (\upsilon_1, 1, 0)^T, p = (p_1, p_2, 0)^T$$

where υ_1 and p_1 are complex parameters uniquely determined by the linear kernels, and the bi-orthogonality normalization condition under the Hermitian inner product is strictly enforced:

$\langle p, q\rangle = \bar{p}^T \cdot q = \bar{p}_1\upsilon_1 + \bar{p}_2 = 1.$

The state vector $X_n = (x_n, y_n, z_n)^T \in \mathbb{R}^3$of the NSFD Tigan system map is decomposed within the local coordinate system of the center manifold W^c. Let $z \in \mathbb{C}$ define the complex coordinates of the two-dimensional critical eigenspace $Y^c = span\{q, \bar{q}\}$. The embedding operator $H\colon \mathbb{C} \to \mathbb{R}^3$ maps the localized flow via the second-order Taylor approximation:

$$X_n = z_n q + \bar{z}_n \bar{q} + W(z_n, \bar{z}_n)$$

where

$$W(z_n, \bar{z}_n) = \frac{1}{2}w_{20}z_n^2 + w_{11}z_n\bar{z}_n + \frac{1}{2}w_{02}\bar{z}_n^2 + \mathcal{O}(|z_n|^3).$$

By substituting the coordinate restrictions into the global map and executing the bi-orthogonal inner product projections with the adjoint left eigenvector $p\epsilon\mathbb{C}^3$ the restricted dynamic tracking equation reduces to the standard Poincaré-Birkhoff normal form:

$$z_{n+1} = \lambda_1 z_{n+1} + \frac{1}{2}g_{20}z_n^2 + g_{11}z_n\bar{z}_n + \frac{1}{2}g_{02}\bar{z}_n^2 + \frac{1}{2}g_{21}z_n^2\bar{z}_n + \mathcal{O}(|z_n|^3).$$

The second-order complex Taylor coefficients $g_{ij}\epsilon\mathbb{C}$ are computed directly from the symmetric bilinear form contractions:

$$\begin{aligned} g_{20}(\varphi_{NS}) &= \langle p, B(q,q)\rangle = \bar{p}^T \cdot \; B(q,q) \\ g_{11}(\varphi_{NS}) &= \langle p, B(q,\bar{q})\rangle = \bar{p}^T \cdot B(q,\bar{q}) \\ g_{02}(\varphi_{NS}) &= \langle p, B(\bar{q},\bar{q})\rangle = \bar{p}^T \cdot \; B(\bar{q},\bar{q}) \\ g_{21}(\varphi_{NS}) &= \langle p, C(q,q,q)\rangle \end{aligned} \tag{23}$$

By some tedious calculation, this coefficients are obtained as g_{20}=0, $g_{11}=0$, $g_{02}=0$ and $g_{21}=-\varphi_{NS}a\bar{p}_2\left[2v_1\left(\frac{v_1+\bar{v}_1}{b}\right)+\bar{v}_1\left(\frac{\varphi_{NS}v_1}{2\lambda_1-1+\varphi_{NS}b}\right)\right]$. To determine the topological stability and orientation of the bifurcating closed invariant curves, we construct the First Lyapunov Coefficient(l_1). By leveraging the fact that $g_{20}=g_{11}=g_{02}=0$, the generalized invariant mapping simplifies to the following analytical kernel:

$$l_1=-\frac{\varphi_{NS}a}{2}Re\left(e^{-i\theta_0}\bar{p}_2\left[2v_1\left(\frac{v_1+\bar{v}_1}{b}\right)+\bar{v}_1\left(\frac{\varphi_{NS}v_1}{2\lambda_1-1+\varphi_{NS}b}\right)\right]\right). \tag{24}$$

Theorem 1: Suppose that the condition (12) is satisfied and $\ell_1(\varphi_{NS})\neq 0$. Then, a Neimark-Sacker bifurcation occurs at the fixed point $E_0(0,0,0)$ of system (2) when the bifurcation parameter φ passes through the critical value φ_{NS}. Moreover, if $\ell_1(\varphi_{NS})<0$,the bifurcation is supercritical and a stable invariant closed curve emerges from E_0; whereas if resp. $\ell_1(\varphi_{NS})>0$, the bifurcation is subcritical and an unstable invariant closed curve is generated.

3.1.2. Neimark-Sacker bifurcation around E_+

In this section, the localized bifurcation dynamics of the 3D Tigan system discretized via the Non-Standard Finite Difference (NSFD) scheme (2) are investigated. The critical threshold of the step-size parameter φ, where the system loses its asymptotic stability and transitions into a stable limit cycle, is rigorously analyzed by employing the Lemma 5.

For n=3, the following lemma establishes the necessary and sufficient parametric conditions under which System (2) undergoes a Neimark–Sacker bifurcation as the bifurcation parameter crosses its critical value.

Lemma 6: System (2) undergoes a Neimark–Sacker bifurcation near the fixed point E_0 at $\varphi=\varphi_{NS}$ if and only if the following conditions hold:

$$\begin{aligned}
&1-\kappa_1+\kappa_0(\kappa_2-\kappa_0)=0\\
&1+\kappa_1-\kappa_0(\kappa_2+\kappa_0)>0\\
&1+\kappa_2+\kappa_1+\kappa_0>0\\
&1-\kappa_2+\kappa_1-\kappa_0>0\\
&\frac{d}{d\varphi}\left(1-\kappa_1+\kappa_0(\kappa_2-\kappa_0)\right)_{\varphi=\varphi_{NS}}\neq 0\\
&cos\left(\frac{2\pi}{\ell}\right)\neq 1-\frac{1+\kappa_2+\kappa_1+\kappa_0}{2(1+\kappa_0)},\ell=3,4,5,\ldots
\end{aligned}$$

where $\kappa_2,\kappa_1,\kappa_0$ are given as in (12).

Set

$$NSB_{E_2}=\{(a,b,c,\varphi):\varphi=\varphi_{NS},a,b,c>0\ \}$$

and for parameter perturbation in a small neighborhood of NSB_{E_+} two roots of (12) equation are complex conjugate having modulus one and magnitude of other root is not equal to one, then the system (2) experiences Neimark-Sacker bifurcation around E_+ as given:

$$\varphi_{NSB_{E_2}} = \frac{1}{6(-c+a)ab}\sqrt[3]{b^2\left(H + 12a\sqrt{-\frac{1}{ab}\mathrm{K}}\right)} + \frac{L}{3((-c+a)a)\Theta} + \frac{2(2a-c)}{3a(-c+a)} \qquad (25)$$

$$\mathrm{H} = 648a^4 + 944a^3b - 972a^3c - 1020a^2bc + 324a^2c^2 + 204abc^2 + 8bc^3$$

$$\begin{aligned}\mathrm{K} = 3(&108a^8 - 72a^7b - 324a^7c - 332a^6b^2 + 432a^6bc + 324a^4c^2 \\ &+ 252a^5b^3 + 1008a^5b^2c - 855a^5bc^2 - 108a^5c^3 \\ &- 820a^4b^3c - 1174a^4b^2c^2 + 702a^4bc^3 + 989a^3b^3c^3 \\ &+ 628a^3b^2c^3 - 207a^3bc^4 - 510a^2b^3c^3 - 114a^2b^2c^4 \\ &+ 113ab^3c^4 - 16ab^2c^5 - 16b^3c^5\end{aligned}$$

$$\mathrm{L} = 2(9a^3 + 25a^2\mathrm{b} - 9a^2\mathrm{c}) - 19\mathrm{abc} + \mathrm{b}c^2.$$

Set

$$NSB_{E_+} = \{(a, b, c, \varphi): \varphi = \varphi_{NS}, a, b, c > 0\ \}$$

and for a parameter perturbation in a small neighborhood of NSB_{E_+}, two roots of (11) are complex conjugate having modulus one and the magnitude of other root is not equal to one, the system (2) experiences NS bifurcation around E_+. Let $\kappa_1, \kappa_2 \epsilon \mathbb{C}^3$ be the right and left eigenvectors of $A(\varphi_{NS})$, respectively, corresponding to the critical conjugate eigenvalues $\rho_1(\varphi_{NS})$ and $\rho_2(\varphi_{NS})$, such that

$$A(\varphi_{NS})\kappa_1 = \rho_1(\varphi_{NS})\kappa_1, A^T(\varphi_{NS})\kappa_2 = \rho_2(\varphi_{NS})\kappa_2 \; and < \kappa_2, \kappa_1 >= \sum_{i=1}^{3} \bar{\kappa}_{2i}\kappa_{1i} = 1$$

The coefficient $\ell_2(\varphi_{NS})$, obtained from equation (24), characterizes both the direction and the stability of the Neimark–Sacker bifurcation. The corresponding results are stated in the following theorem.

Theorem 2: Suppose that condition (12) holds and $\ell_2(\varphi_{NS}) \neq 0$. Then the positive equilibrium point E_+ of system (2) experiences a Neimark–Sacker bifurcation when the parameter φ crosses the critical threshold φ_{NS}. In addition, if $\ell_2(\varphi_{NS}) < 0$, the bifurcation is supercritical and gives rise to an attracting invariant closed curve in a neighborhood of E_+. On the other hand, if $\ell_2(\varphi_{NS}) > 0$, the bifurcation is subcritical and an unstable invariant closed curve is generated near E_+.

4. Numerical Simulations

In this section, comprehensive numerical experiments to validate the theoretical bifurcation thresholds and normal form classifications derived in the previous sections are presented. The simulations illustrate how the Non-Standard Finite

Difference (NSFD) scheme behaves under different step-size parameters φ across two distinct parametric regimes.

Case 1: Parameter values are taken as $a = 12, b = 8, c = 4$. By some calculation, the bifurcation point is obtained as $\varphi_{NS} = 0{,}125$ at fixed point $E_0(0,0,0)$ of the system (2). The Jacobian matrix at E_0 have eigenvalues $\rho_1 = 0.5$ and $\rho_{2,3} = 0.7 \pm 0.714142842854285i$ with $|\rho_i| = 1, i = 2{,}3$. Furthermore

$$\frac{d|\rho_i(\varphi)|}{d}\Big|_{\varphi=\varphi_{NS}} = \frac{a(a-c)}{2(2a-c)} = 2.4 \neq 0, i = 2{,}3.$$

$$\frac{a}{a-c} = \frac{3}{2} \neq -2, -\frac{3}{2}.$$

Therefore, the conditions for the existence of a Neimark–Sacker bifurcation are satisfied for $(a, b, c, \varphi) \epsilon NSBE_0$, which confirms Lemma 3. Consequently, a Neimark–Sacker bifurcation occurs in a neighborhood of the fixed point E_0 as the parameter φ crosses its critical value φ_{NS}.

Let $q_1, p_1 \epsilon \mathbb{C}^3$ be eigenvectors of $A(\varphi_{NS})$ and $A^T(\varphi_{NS})$ corresponding to the eigenvalues corresponding to $\rho_{1,2}$ respectively. By straightforward algebraic computations, the eigenvectors are obtained as follows:

$q_1 \sim (0.5 - 1.190238i, 1{,}0)^T$, and $p_2 \sim (1, -0.3 - 0.7141428i)^T$. Calculating the coefficient g_{20}, g_{21}, g_{11} and g_{02} with (23), The Lyapunov coefficient $l_1(\varphi_{NS}) < 0$. So, the NS bifurcation is supercritical according to the Theorem 1.

The NS diagram are displayed in Figure 1(i) which reveal that the conditions of stability for the fixed point E_0 occurs when $\varphi < \varphi_{NS}$, loses its stability at $\varphi = \varphi_{NS}$ and there appears an attracting closed invariant curve when $\varphi > \varphi_{NS}$. The MLEs related Figure1(i) are shown Figure 1(ii). The phase portraits of system (2) are plotted for different values of φ in Figure 2.

Case 2: By taking $a = 10, b = 8$ and $c = 28$. the positive fixed point is found as $E_+ = (3.7947331922, 3.7947331922, 1.8)$ of system and bifurcation parameter $\varphi_{NS_+} = 0.01278893113$. The Jacobian matrix is obtained at E_+ as

$$A(\varphi_{NS}) = \begin{pmatrix} 0.8866118246 & 0.1133881756 & 0 \\ 0 & 1 & -0.48530581464 \\ 0.04402619739 & 0.04402619739 & 0.9071846264 \end{pmatrix},$$

and the eigenvalues of $A(\varphi_{NS})$ are $\rho_{1,2} = 0.9864774997 \mp 0.1638967173i$, $\rho_3 = 0.8208414516$ with $|\rho_{1,2}| = 1$. Furthermore

$$1 - \kappa_1 + \kappa_0(\kappa_2 + \kappa_0) = 0$$

$$1 + \kappa_1 - \kappa_0(\kappa_2 + \kappa_0) = 0.652438648 > 0$$

$$1 + \kappa_2 + \kappa_1 + \kappa_0 = 0.0048453427 > 0$$

$$1 - \kappa_2 + \kappa_1 - \kappa_0 = 7.234121133 > 0$$
$$1 + \kappa_0 = 0.1791585557 > 0$$
$$1 - \kappa_0 = 1.820841444 > 0$$
$$\frac{\partial}{\partial \varphi}\left(1 - \kappa_1 + \kappa_0(\kappa_2 - \kappa_0)\right) \neq 0$$

and

$$1 - \frac{1+\kappa_2+\kappa_1+\kappa_0}{2(1+\kappa_0)} = 0.98647750122.$$

From the resonance condition $cos\left(\frac{2\pi}{l}\right) = 0.98647750122$, we get $l = \pm 6.36931435274$.

By Lemma 6, the transversality and non-resonance conditions required for a Neimark–Sacker bifurcation are satisfied at E_+. Hence, the system exhibits a Neimark–Sacker bifurcation at the fixed point φ_{NS} when $\varphi = \varphi_{NS}$, and an invariant closed curve is generated in a neighborhood of E_+.

Let $m_1, m_2 \epsilon \mathbb{C}^3$ denote the right and left eigenvectors of $A(\varphi_{NS})$ associated with the critical eigenvalues $\rho_{1,2}$ respectively. These eigenvectors are computed explicitly as follows:

$m_1 \sim (-0.2541 - 0.4170i, 0.8265, 0.0230 - 0.2791)^T$,$m_2 \sim (0.1093 + 0.1793i, -0.1496 + 0.3091i, 09154)^T$. For $< m_1, m_2 > = 1$, normalized vector is taken as $m_2 \sim (0.2380 - 0.2486i, 0.5417 + 0.1139i, -0.3556 - 1.4319i)^T$. Calculating the coefficient g_{20}, g_{21}, g_{11} and g_{02} with (23), The Lyapunov coefficient $l_1(\varphi_{NS}) > 0$. So, the NS bifurcation is subcritical according to the Theorem 2.

Figure 3(i), shows the Neimark–Sacker bifurcation diagram for $a = 10, b = 8$ and $c = 28$, where the critical bifurcation value is $\varphi_{NS_+} = 0.01278893113$ at the equilibrium point $E_+ = (3.7947331922, 3.7947331922, 1.8)$. The bifurcation diagram is represented in the (x, y, z) −space. Figure 4-5 depicts the corresponding phase portraits of System (2) for several values of φ, illustrating the evolution of the system dynamics before and after the onset of the Neimark–Sacker bifurcation. Figure (6) illustrates chaotic attractor and the corresponding Poincaré section of system (2) in the (x, y, z) −space and (x, y, z) −plane, respectively, demonstrating the chaotic dynamics around the equilibrium point E_+.

Case 3: By taking $a = 2, b = 0.4$ and $c = 5$ the positive fixed point is found as $E_+ = (0.7745966692, 0.7745966692, 1.5)$ of system and bifurcation parameter $\varphi_{NS_+} = 0.047815$. The Jacobian matrix is obtained at E_+ as

$$A(\varphi_{NS}) = \begin{pmatrix} 0.9131064341 & 0.08689356591 & 0 \\ 0 & 1 & -0.07371261905 \\ 0.03616794258 & 0.03616794258 & 0.9813229552 \end{pmatrix},$$

and the eigenvalues of $A(\varphi_{NS})$ are $\rho_{1,2} = 1.00033816443896 \mp 0.066035538269995i$, $\rho_3 = 0.893753060422073$ with $|\rho_{1,2}| = 1$. Furthermore

$$1 - \kappa_1 + \kappa_0(\kappa_2 + \kappa_0) = 0$$
$$1 + \kappa_1 - \kappa_0(\kappa_2 + \kappa_0) = 0.386349936 > 0$$
$$1 + \kappa_2 + \kappa_1 + \kappa_0 = 0.0004633218 > 0$$
$$1 - \kappa_2 + \kappa_1 - \kappa_0 = 7.585832136 > 0$$
$$1 + \kappa_0 = 0.1017449838 > 0$$
$$1 - \kappa_0 = 1.898255016 > 0$$
$$\frac{\partial}{\partial \varphi}\left(1 - \kappa_1 + \kappa_0(\kappa_2 - \kappa_0)\right) \neq 0$$

and

$$1 - \frac{1+\kappa_2+\kappa_1+\kappa_0}{2(1+\kappa_0)} = 0.9977231222.$$

From the resonance condition $cos\left(\frac{2\pi}{l}\right) = 0.9977231222$, we get $l = \pm 6.29752399977$.

In view of Lemma 6, the necessary and sufficient conditions for the existence of a Neimark–Sacker bifurcation are fulfilled for $(a, b, c, \varphi) \in NSB_{E_2}$. Hence, the fixed point E_+ experiences a Neimark–Sacker bifurcation as the parameter φ crosses the critical threshold φ_{NS}.

Let $t_1, t_2 \epsilon \mathbb{C}^3$ be two eigenvectors of $A(\varphi_{NS})$ and $A^T(\varphi_{NS})$ corresponding to $\rho_{1,2}$ respectively. By some algebraic calculation t_1, t_2 can be found as follows, $t_1 \sim (0.405941170103580 - 0.307302670365212i, 0.6410583723889, -0.0029409231097 - 0.57429291251)^T$ and $t_2 \sim (-0.18739031 + 0.14185686i, 0.183402262868 + 0.63691474i, -0.710960419)^T$.

Some calculation via help of (17) MLEs is obtained positive. So, according to the theorem, the Neimark-Sacker bifurcation is subcritical.

Figure 7(i) presents the Neimark–Sacker bifurcation diagram and the corresponding maximum Lyapunov exponents (MLEs) of System (2) for a=2, b=0.4,c=5 in the (φ, x)-plane. The critical bifurcation value is found to be $\varphi_{NS_+} = 0.047815$ at the equilibrium point $E_+ = (0.7745966692, 0.7745966692, 1.5)$. Figure 8 depicts the corresponding

phase portraits for several values of φ, illustrating the evolution of the system dynamics as the bifurcation parameter varies. Furthermore, Figure 9 shows the phase portraits of System (2) in the (x, y), (x, z) and (y, z)-planes, respectively, confirming the presence of chaotic dynamics in the vicinity of the equilibrium point E_+.

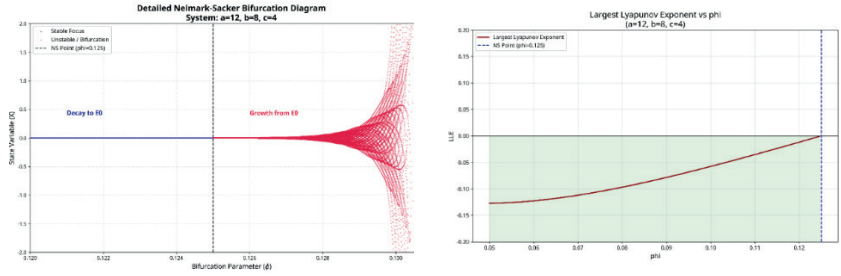

(i) (ii)

Figure 1: (i) Neimark-.sacker Bifurcation Diagram with respect to phi for a=12, b=8 and c=4(ii) Corresponding Maximum Lyapunov Exponents

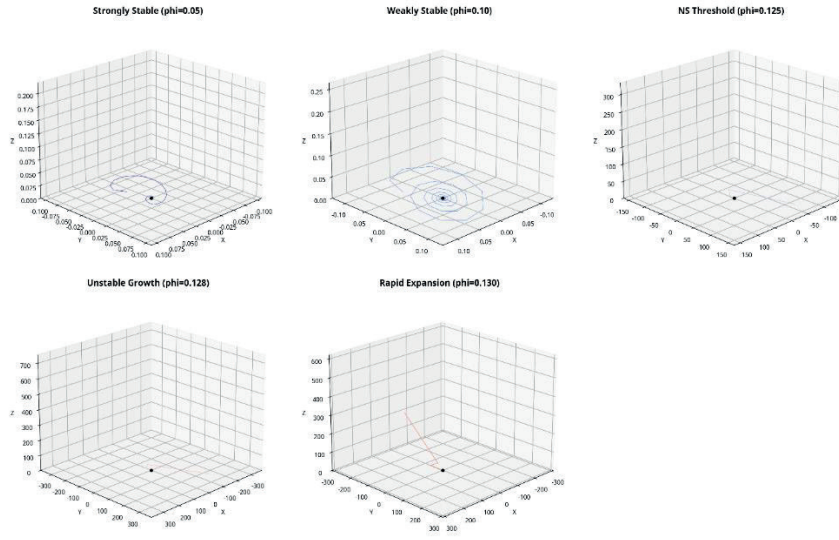

Figure 2:Phase Portraits of System (2) with a=12, b=8,c=4 in (x, y, z) plane for different φ values.

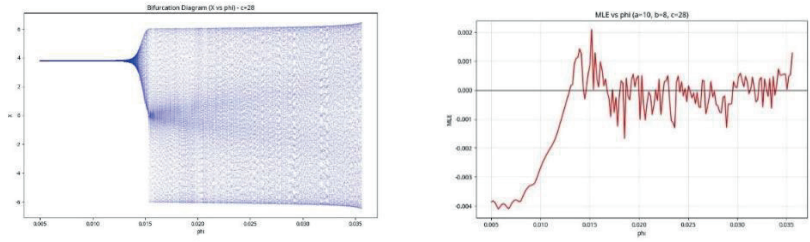

(i) (ii)

Figure 3:Neimark Sacker Bifurcation Diagram with a=10, b=8,c=28 in (φ, x) plane and MLEs.

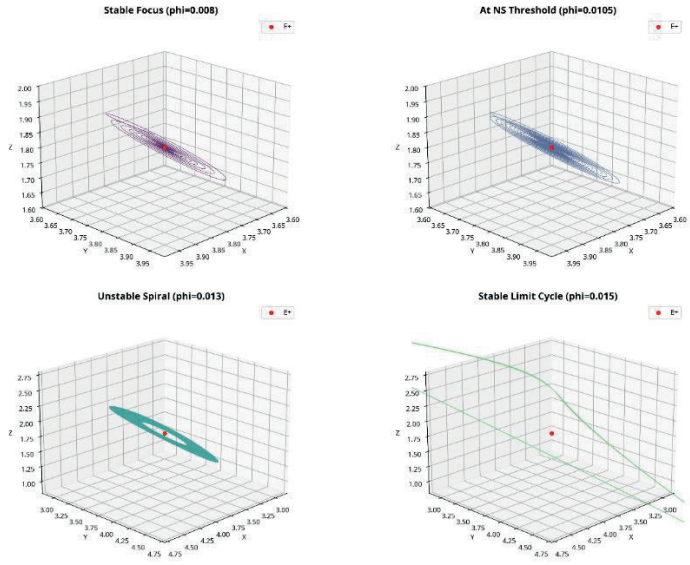

Figure 4: Phase Portraits of System (2) with a=10, b=8,c=28 in (x, y, z) plane for different φ values.

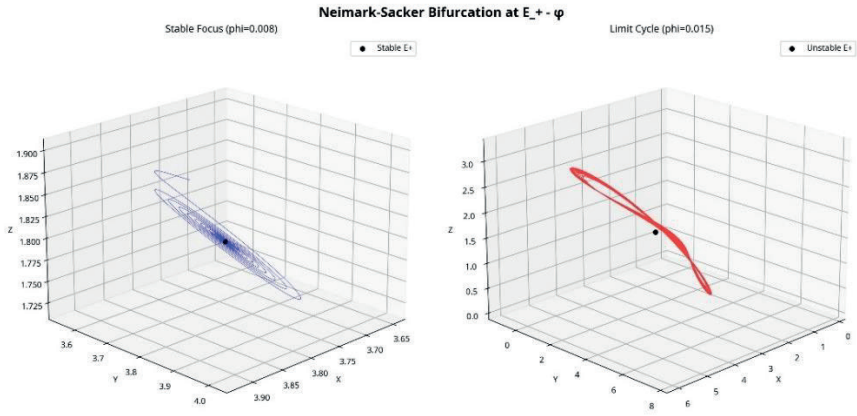

Figure 5:Neimark Sacker Bifurcation Diagram with a=10, b=8,c=28 in (x, y, z) plane.

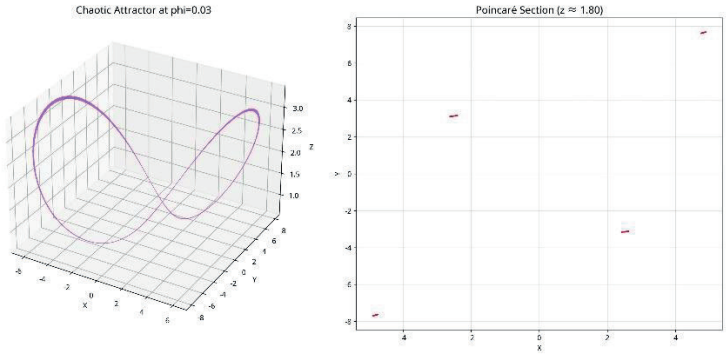

Figure 6: Chaotic attractor in the (x, y, z)-space and its corresponding Poincaré section in the (x, y, z) $-$plane for the equilibrium point E_+ with a=10, b=8,c=28.

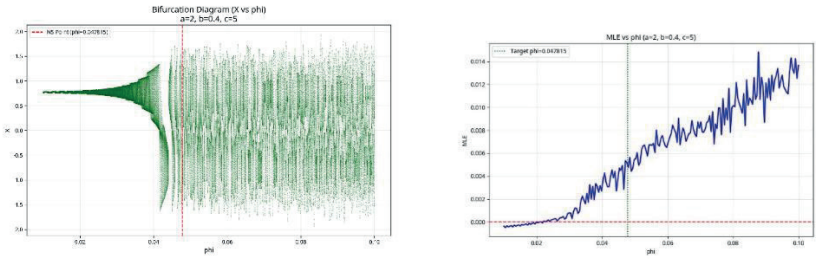

(i) (ii)

Figure 7:Neimark Sacker Bifurcation Diagram with a=2, b=0.4,c=5 in (φ, x) plane and MLEs.

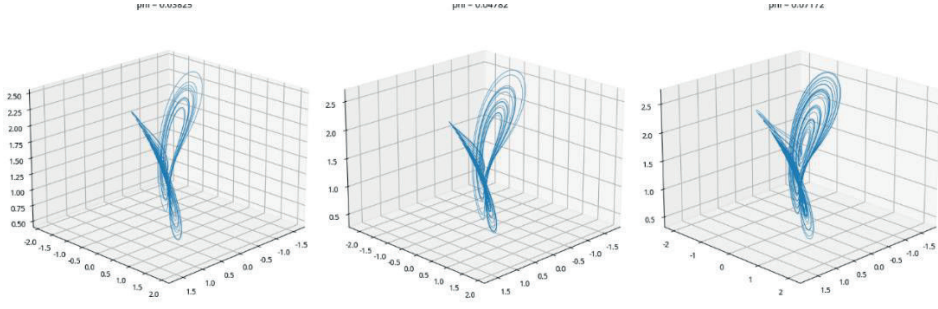

Figure 8: Phase Portraits of System (2) with a=2, b=0.4, c=5 in (x, y, z) plane for different φ values.

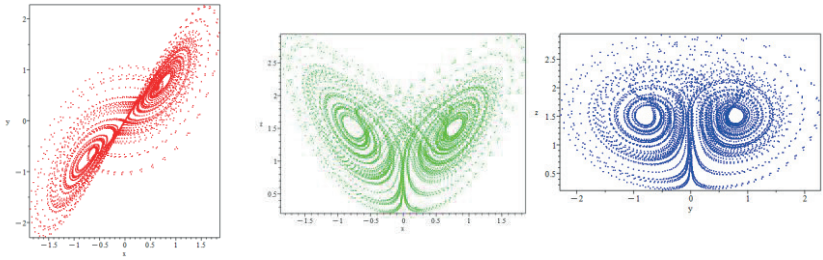

Figure 9: Phase Portraits of System (2) with a=2, b=0.4, c=5 in (x, y), (x,z) and (y,z) plane $\varphi = 0.0475815$ value.

5. Conclusion

In this study, the discrete-time dynamics and bifurcation behaviors of a three-dimensional Tigan system are comprehensively investigated. Instead of employing traditional discretization schemes such as the standard Euler method,which often introduce numerical instabilities and artificial chaos, Non-Standard Finite Difference (NSFD) scheme is utilized to construct a topologically consistent discrete model. This approach successfully preserved the essential structural properties and positivity of the original continuous system.

The primary focus of our mathematical analysis was centered on the local stability and the occurrence of a Neimark-Sacker bifurcation at the positive equilibrium point. By choosing the step size φ as the main bifurcation parameter, we rigorously determined the critical thresholds where the system transitions from a stable steady state to quasi-periodic oscillations. The topological classification and existence conditions for the Neimark-Sacker bifurcation were explicitly derived using Yao's bifurcation criteria, alongside the evaluation of the first Lyapunov coefficient to determine the direction and stability of the emerging invariant closed curve.

To validate the theoretical framework, extensive numerical simulations—including bifurcation diagrams, Lyapunov exponent spectra, and phase portraits—were presented. The numerical results demonstrated an excellent agreement with our analytical findings, confirming that the step size φ plays a crucial role in controlling the complex, chaotic dynamics of the system.

In conclusion, the application of the NSFD method combined with rigorous bifurcation analysis provides a robust framework for understanding and predicting the long-term behavior of 3D chaotic systems in a discrete domain. Future research directions may include the exploration of global bifurcations, chaos control strategies, or the extension of this methodology to fractional-order discrete Tigan systems.

6. References

[1] Camouzis, E., & Ladas, G. (2007). Dynamics of third-order rational difference equations with open problems and conjectures. Chapman and Hall/CRC.

[2] Ciesielski, K. (2012). The Poincaré-Bendixson theorem: from Poincaré to the XXIst century. Central European Journal of Mathematics, 10(6), 2110-2128.

[3] Çetinkaya, İ. T., Kocabıyık, M., & Ongun, M. Y. (2021). Stability analysis of discretized model of glucose–insulin homeostasis. *Celal Bayar University Journal of Science*, *17*(4), 369-377.

[4] Din, Q., Elsadany, A. A., & Khalil, H. (2017). Neimark-Sacker Bifurcation and Chaos Control in a Fractional-Order Plant-Herbivore Model. *Discrete Dynamics in Nature and Society*, *2017*(1), 6312964.

[5] Feng, G., Yin, D., & Jiacheng, L. (2021). Neimark–Sacker Bifurcation and Controlling Chaos in a Three-Species Food Chain Model through the OGY Method. *Discrete Dynamics in Nature and Society*, *2021*(1), 6316235.

[6] He, Z., & Lai, X. (2011). Bifurcation and chaotic behavior of a discrete-time predator–prey system. *Nonlinear Analysis: Real World Applications*, *12*(1), 403-417.

[7] Kangalgil, F., & Işık, S. (2020). Controlling chaos and Neimark-Sacker bifurcation in a discrete-time predator-prey system. *Hacettepe Journal of Mathematics and Statistics*, *49*(5), 1761-1776.

[8] Kocabıyık, M., & Ongun, M. Y. (2023). Discretization and stability analysis for a generalized type nonlinear pharmacokinetic models. *Gazi University Journal of Science*, *36*(4), 1675-1691.

[9] Kocabiyik, M., & Ongun, M. Y. (2025). Distributed order hantavirus model and its nonstandard discretizations and stability analysis. *Mathematical Methods in the Applied Sciences*, *48*(2), 2404-2420.

[10] Kulenović, M. R., Moranjkić, S., Nurkanović, M., & Nurkanović, Z. (2018). Global Asymptotic Stability and Naimark-Sacker Bifurcation of Certain Mix Monotone Difference Equation. *Discrete Dynamics in Nature and Society*, *2018*(1), 7052935.

[11] Kuznetsov, Y. A. (1998). *Elements of applied bifurcation theory*. New York, NY: Springer New York.

[12] Li, X. F., Chu, Y. D., Zhang, J. G., & Chang, Y. X. (2009). Nonlinear dynamics and circuit implementation for a new Lorenz-like attractor. *Chaos, Solitons & Fractals*, *41*(5), 2360-2370.

[13] Liu, W., & Jiang, Y. (2020). Flip bifurcation and Neimark–Sacker bifurcation in a discrete predator–prey model with harvesting. *International Journal of Biomathematics*, *13*(01), 1950093.

[14] Lorenz, E. N. (1963). Deterministic nonperiodic flow, journal of the atmospheric sciences vol. 20. *No. In. XX*.

[15] Luo, W., Ou, Q., Yu, F., Cui, L., & Jin, J. (2020). Analysis of a new hidden attractor coupled chaotic system and application of its weak signal detection. *Mathematical Problems in Engineering*, *2020*(1), 8849283.

[16] E. Mickens, R. (1994). *Nonstandard finite difference models of differential equations*.

[17] Mickens, R. E. (2002). Nonstandard finite difference schemes for differential equations. *Journal of Difference Equations and Applications*, *8*(9), 823-847.

[18] Kocabıyık, M. (2022). Nonstandard discretization and stability analysis of a novel type Malaria-Ross model. Journal of the Institute of Science and Technology, 12(2), 1023-1033.

[19] Qin, S., Zhang, J., Du, W., & Yu, J. (2016). Neimark–sacker bifurcation in a new three–dimensional discrete chaotic system. *ICIC-EL*, *10*(4), 1-7.

[20] Rana, S. M. S. (2023). Bifurcation analysis and 0-1 chaos test of a discrete T system. *Chaos Theory and Applications*, *5*(2), 90-104.

[21] Rössler, O. E. (1976). An equation for continuous chaos. *Physics Letters A*, *57*(5), 397-398.

[22] Jury, E. I. (1962). A simplified stability criterion for linear discrete systems. *Proceedings of the IRE*, *50*(6), 1493-1500.

[23] Tigan, G. (2005). Analysis of a dynamical system derived from the Lorenz system. *Sci. Bull. Politehnica Univ. Timisoara Tomul*, *50*(64), 61-72.

[24] Wen, G. (2005). Criterion to identify Hopf bifurcations in maps of arbitrary dimension. *Physical Review E—Statistical, Nonlinear, and Soft Matter Physics*, *72*(2), 026201.

[25] Xin, B., Chen, T., & Ma, J. (2010). Neimark-Sacker Bifurcation in a Discrete-Time Financial System. *Discrete Dynamics in Nature and Society*, *2010*(1), 405639.

[26] Yao, S. (2012). New bifurcation critical criterion of Flip-Neimark-Sacker bifurcations for two-parameterized family of n-dimensional discrete systems. *Discrete Dynamics in Nature and Society*, *2012*(1), 264526.

[27] Yousef, A. M., Salman, S. M., & Elsadany, A. A. (2018). Stability and bifurcation analysis of a delayed discrete predator–prey model. *International Journal of Bifurcation and Chaos*, *28*(09), 1850116.

[28] Yousef, A. M., Rida, S. Z., & Arafat, S. (2020). Stability, analytic bifurcation structure and chaos control in a mutual interference host-parasitoid model. *International Journal of Bifurcation and Chaos*, *30*(15), 2050237.

[29] Zhang, Y., Cheng, Q., & Deng, S. (2023). Qualitative structure of a discrete predator-prey model with nonmonotonic functional response. *Discrete & Continuous Dynamical Systems-Series S*, *16*.

[30] Zhao, M. (2021). Bifurcation and chaotic behavior in the discrete BVP oscillator. *International Journal of Non-Linear Mechanics*, *131*, 103687.